THE ASTRONOMICAL JOURNAL VOLUME 114, NUMBER 6 DECEMBER 1997

POST-MAXIMUM OPTICAL AND INFRARED OBSERVATIONS OF NOVA V1425 AQUILAE 1995

U. S. KAMATH
Physical Research Laboratory, Navarangpura, Ahmedabad 380 009, India
Electronic mail: kamath@prl.ernet.in

G. C. ANUPAMA
Indian Institute of Astrophysics, Bangalore 560 034, India
Electronic mail: gca@iiap.ernet.in

N. M. ASHOK AND T. CHANDRASEKHAR
Physical Research Laboratory, Navarangpura, Ahmedabad 380 009, India
Electronic mail: ashok@prl.ernet.in, chandra@prl.ernet.in

Received 1997 June 3; revised 1997 August 25; accepted 1997 August 26

ABSTRACT

We present the post-maximum optical spectroscopy and infrared photometry of Nova V1425 Aquilae 1995. The data indicate that the nova belongs to the Fe II class and that it formed an optically thin dust shell at a very early phase compared to other dust forming novae of the same class. The total dust mass is very low with a dust-to-gas ratio of $\lesssim 10^{-3}$. The optical spectrum and its evolution are similar to other Fe II novae. An extinction of $E_{B-V}=0.76$ is derived from the He I line ratios and a distance of 2.7 kpc is estimated from the magnitude-decay time relations. © *1997 American Astronomical Society.* [S0004-6256(97)01712-3]

1. INTRODUCTION

Nova V1425 Aquilae 1995 was discovered on 1995 February 7.84 UT by K. Takamizawa (Nakano 1995), at a magnitude of 8.1. Early spectroscopic observations by Wagner *et al.* (1995), Ohshima *et al.* (1995) and Iijima *et al.* (1995) indicate that the nova was discovered well after maximum. The presence of strong, permitted Fe II emission lines and the FWHM velocity of ~ 1300 km s^{-1} indicate the nova belongs to the "Fe II" class of novae. The "Fe II" class of novae (Williams 1992) exhibit lines due to low ionization transitions, with Fe II lines as the strongest non-Balmer lines in the spectrum during the early post-maximum phases. These novae also have low expansion velocities ($\leqslant 2500$ km s^{-1}). Infrared photometry of the nova by Mason *et al.* (1996, hereafter M96) revealed the existence of an optically thin dust shell. The development of V1425 Aql was found to be very similar to that of V1668 Cygni. Based on this similarity, M96 estimate the outburst occurred around 1995 January 21–29 UT (JD 2 449 742.5±4.0), with a maximum apparent magnitude of $(m_v)_{\max}\sim 6.2$ and a rate of decline $t_2=11$ days. Ultraviolet spectra (Greeley *et al.* 1995) indicate an extinction of $E_{B-V}\geqslant 0.56$. M96 estimate the distance to the nova to be 3.6–4.8 kpc.

We describe in this paper the results obtained based on optical spectroscopic observations of V1425 Aql between 1995 March 15–1995 May 18, 1997 May 17 and *JHK* photometry between 1995 February 15–May 18.

2. THE OPTICAL SPECTRUM

CCD spectra of the nova were obtained with a resolution of 4.5 Å/pixel in the wavelength range 4400–7100 Å on 1995 March 15, 16, April 7, and May 18. All data were obtained using the Boller & Chivens spectrograph at the Cassegrain focus of the 2.3 m telescope at the Vainu Bappu Observatory, Kavalur. A single spectrum at a resolution of 5.3 Å/pixel in the wavelength range 4200–8200 Å was obtained on 1997 May 17, more than two years after outburst, using the OMR spectrograph on the 2.3 m telescope (Prabhu *et al.* 1997). All data were reduced in the standard method using the reduction packages available under IRAF. The spectra are flux calibrated using spectrophotometric standard stars. Since the sky conditions were non-photometric, zero point corrections to the observed fluxes were applied using *V* magnitudes reported in the IAU circulars and the variable star network (VSNET). Since no *V* magnitude estimate was available for 1997 May 17, zero point correction has not been applied to that spectrum.

The spectra presented here cover four epochs: 1995 March 15–16 (Epoch I); 1995 April 7 (Epoch II), 1995 May 18 (Epoch III), and 1997 May 17 (Epoch IV). Figures 1(a) and 1(b) show the spectrum in each of these epochs. At all epochs the spectra show strong emission lines. The spectra during the first three epochs are characteristic of a nova spectrum during early decline, while the spectrum during the last epoch is that of a nova in the nebular stage. The line identifications and the observed fluxes relative to Hβ are listed in Tables 1 and 2. The spectral development is consistent with

 0004-6256/97/114(6)/2671/8/$10.00

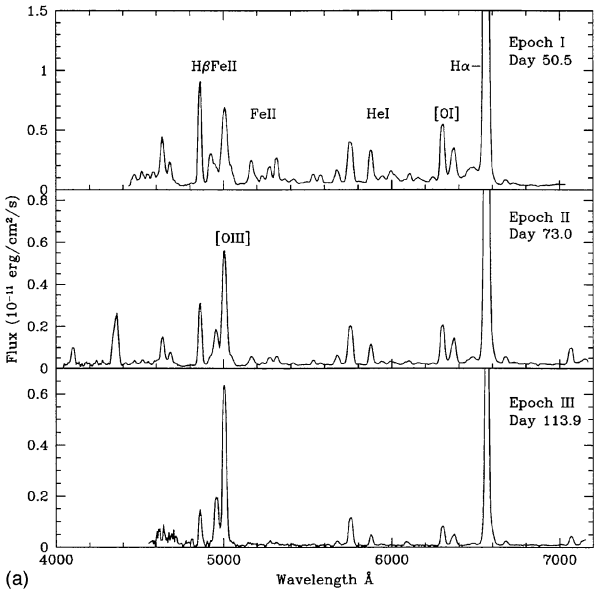

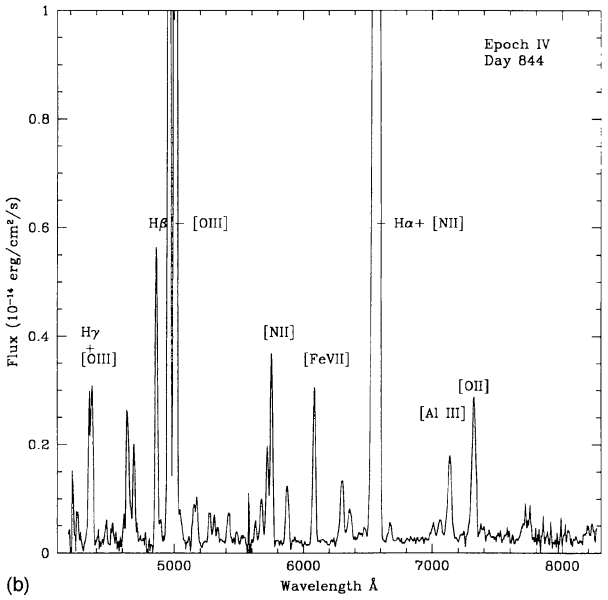

FIG. 1. (a) Optical spectrum of V1425 Aql on 1995 March 15–16 (Epoch I, top), April 7 (Epoch II, middle), and May 18 (Epoch III, bottom). (b) Spectrum of V1425 Aql in the nebular phase (1997 May 17: Epoch IV).

the "Fe II" classification of the nova. The nova was in the A_o phase (CTIO classification scheme: Williams *et al.* 1991) during the first three epochs and in the phase N_o during Epoch IV. The spectrum at each epoch is briefly described below.

Epoch I: Hydrogen Balmer lines, permitted Fe II and N II lines are present in the spectrum. The [O I] 5577, 6300, and 6364 Å lines are fairly strong. [O III] 4959 and 5007 Å lines are also strong, blended with Fe II lines. Helium lines were also strong. The spectrum during this epoch is similar to that of nova V443 Scuti 1989, 72 days after outburst (Anupama *et al.* 1992) and nova V1819 Cygni 1986, 92 days after outburst (Whitney & Clayton 1989). The strength of the helium

TABLE 1. Early spectra: Line identification and observed fluxes relative to Hβ.

λ		$F_\lambda/F_{H\beta}$			
(Å)	Species	day 49.98	50.97	73.0	113.9
4101	Hδ	...	...	0.287	...
4173	Fe II(27)	...	...	0.074	...
4233	Fe II(27)	...	...	0.066	...
4340	Hγ	...	...	0.366	...
4363	[O III]	...	...	0.715	...
4417	Fe II(27)	...	...	0.050	...
4447	N II(15)	...	0.054	0.041	...
4471	He I	0.151	0.084	0.065	...
4515	Fe II(37)	0.203	0.190	0.104	...
4556	Fe II(37)	0.167	0.209	0.071	...
4584	Fe II(38)	0.205	0.198	0.096	...
4640	N/O blend	0.606	0.613	0.549	...
4686	He II	0.254	0.282	0.264	...
4826	Fe II(37)	0.017	0.019	0.018	...
4861	Hβ	1.000	1.000	1.000	1.000
4924	Fe II(42)	0.391	0.352	0.271	0.121
4959	[O III]	0.215	0.244	0.670	1.970
5007	[O III]	1.226	1.276	2.456	5.510
5047		0.152	0.166	0.199	0.092
5116		0.023	0.023	0.014	0.034
5168	Fe II(42)	0.292	0.298	0.195	...
5199	Fe II(49)	0.077	0.074	...	...
5235	Fe II(49)	0.084	0.126	0.064	0.064
5276	Fe II(49)	0.198	0.253	0.178	0.176
5317	Fe II(49)	0.287	0.319	0.181	0.127
5363	Fe II(48)	0.039	0.089	0.070	0.032
5414	Fe II(48) +	0.068	0.043	0.055	0.127
5411	He II				
5496	N II(29)	0.015	0.016	0.021	0.025
5535	Fe II(55)	0.102	0.098	0.079	0.079
5577	[O I](3)	0.089	0.083	0.036	0.034
5680	N II(3)	0.164	0.165	0.199	0.183
5755	[N II](3)	0.628	0.624	0.902	1.152
5814		0.019	0.015	0.020	0.030
5876	He I	0.397	0.351	0.361	0.183
5896	Na I(1)	0.042	0.603	0.032	...
5942	N II(28)	0.097	0.065	0.076	...
5991	Fe II(46)	0.126	0.109	0.037	0.020
6019		0.084	0.088	0.078	0.017
6084	Fe II(46)	0.022	0.020	0.033	0.184[1]
6108	Fe II(46)	0.088	0.092	0.056	0.036
6147	Fe II(74)	0.025	0.011	...	0.017
6162	O I(10)	0.026	0.044	0.036	...
6181		0.025	0.014	0.013	...
6248	Fe II(74)	0.066	0.058	0.026	0.019
6300	[O I] (1)	0.805	0.747	0.830	0.768
6364	[O I] (1)	0.572	0.504	0.594	0.460
6455	Fe II (74)	0.565	0.495	0.248	0.212
6563	Hα	sat	18.410	15.330	10.560
6678	He I	0.195	0.187	0.147	0.139
6730		0.105	0.131	0.033	...
6830		0.020	0.015	0.028	0.025
7065	He I	...	...	0.387	0.374
		$F_{H\beta}$ (10^{-11} ergs/cm²/s)			
		2.254	3.049	2.781	0.733

[1]Contribution from [Fe VII] 6087.

lines in V1425 Aql are however much stronger than in V443 Sct and V1819 Cyg. The spectrum of V1425 Aql on the other hand compares very well with the 1991 June 12 (Δt ~64 days) spectrum of Nova Ophiuchi 1991, also an

TABLE 2. Nebular spectra: Line identification and observed fluxes relative to Hβ.

λ (Å)	Species	$F_\lambda/F_{H\beta}$ day 843.8
4266	[Fe II]	0.041
4277	[Fe II]	0.052
4340	Hγ	0.441
4363	[O III]	0.492
4635	[N III]	0.537
4686	He II	0.303
4861	Hβ	1.000
4959	[O III]	8.497
5007	[O III]	25.279
5047	He I	0.147
5158	[Fe VIII]	0.171
5177	[Fe VI]	0.144
5276	[Fe VII]	0.135
5309	[Ca V]	0.089
5411	He II	0.132
5631	[Fe VI]	0.067
5674	[Fe VI]	0.169
5755	[N II]	0.657
5876	He I	0.243
6087	[Fe VII], [Ca V]	0.593
6300	[O I]	0.291
6363	[O I]	0.112
6565	Hα+[N II]	14.380
6678	He I	0.066
7007	[Ar V]	0.083
7065	He I	0.110
7136	[Al III]	0.444
7325	[O II]	0.733
7727	[S I]	0.057
7759	[Ar III]+O I	0.116

$F_{H\beta}=1.271\times10^{-14}$ ergs/cm^2/s

"Fe II" nova (Williams *et al.* 1994) which had fairly strong helium lines.

Epoch II: The strength of the Fe II lines has decreased considerably as also the strength of other permitted lines. The [O III] 5007 Å line is stronger than Hβ. The observed He I 5876/4471 line ratio of 5.54 implies a reddening of $E_{B-V}=0.76$.

Epoch III: The permitted iron and nitrogen lines have disappeared. [O III] line strength has further increased. [O I] lines are still present as also the helium lines.

Epoch IV: The spectrum during this epoch is typical of a nova in the nebular stage with strong forbidden and high ionization lines. The strength of [O III] 5007 Å is nearly twenty times that of Hβ. Lines of [Fe VI] and [Fe VII] are also present. Na I D is weakly present in absorption.

3. DATE OF OUTBURST, REDDENING AND DISTANCE

The early spectra of the nova obtained immediately after discovery indicate the nova was past its maximum at the time it was discovered. Based on the similarity of the visual light curve of V1425 Aql with nova V1668 Cygni, M96 estimate the nova was discovered about ~10 days past maximum. They estimate the outburst maximum occurred around 1995 January 20–29 UT with a maximum magnitude of $m_{vis}=6.2$.

TABLE 3. Observed *JHK* magnitudes.

Date UT	JD 2440000+	*J*	*H*	*K*
1995 Feb				
16.02	9764.52	5.93	5.43	4.36
17.02	9765.52	5.96	5.59	4.24
18.02	9766.52	6.14	...	4.45
19.02	9767.52	6.26	5.74	4.44
24.04	9772.54	6.44	6.02	4.51
1995 Mar				
10.01	9786.50	7.18	6.72	5.12
11.02	9787.52	7.22	6.76	5.01
1995 May				
18.93	9856.43	...	...	8.64

As mentioned earlier, the spectrum of V1425 Aql on 1995 March 16 is similar to that of V443 Sct 72 days after outburst maximum. On this day, nova V443 Scuti was 4.2 mag below maximum. Since novae of a similar class broadly have a very similar spectral evolution which closely follows the evolution of the light curve, comparing the two novae and based on the estimate of the V magnitude of V1425 Aql on March 16 of $V=10.38$, we estimate the maximum magnitude as $V=6.2$. This value agrees with the estimate of M96. Extrapolating the V light curve of V1425 Aql linearly in log t (t in Julian Days), we estimate the date of outburst as $JD_{max}=2\,449\,742.70$, in agreement with the estimate of M96. The rate of decline is estimated as $t_2=11$ days and $t_3=23$ days. Using the various maximum magnitude—rate of decline relations using t_2 and t_3 available in the literature (Cohen 1985; Capaccioli *et al.* 1989), we obtain the absolute maximum magnitude as $M_V^{max}=-8.4\pm0.4$, giving a distance modulus of $m-M=14.2$.

The foreground reddening towards V1425 Aql is estimated using various indicators and relations. As mentioned earlier, the He I line ratio gives a reddening of $A_V=2.4$. Greeley *et al.* (1995) give a lower limit to the reddening as $A_V\geqslant1.7$ based on the He II 1640/1085 Å line ratio. The nova lies at $l^{II}=+33.01$ and $b^{II}=-3.90$. The distribution of the interstellar medium in this region is highly patchy with A_V ranging from 2.6 to 3.3 at a distance of 1 kpc (Neckel & Klare 1980). Two old novae, V528 Aql and EU Sct, which lie in the vicinity of the nova are estimated to have $A_V=2.6\pm0.6$ (Duerbeck 1981), while the open clusters NGC 6704 and NGC 6755, both of which lie within a degree of the nova give a limit to the reddening as $0.72\leqslant E_{B-V}\leqslant0.93$.

Our spectroscopic observations correspond to 50.5, 73.0, 113.9, and 843.8 days after outburst. The Hα/Hβ ratio corrected for reddening using $E_{B-V}=0.76$ as estimated using the He I line ratio is 10.0, 6.95 and 4.79 respectively for the first three epochs. These ratios are consistent with the temporal evolution of the Balmer decrement observed in other novae of the "Fe II" class (e.g., V1819 Cyg, Whitney & Clayton 1989; V443 Sct, Anupama *et al.* 1992).

Based on the above arguments, we assume a value of $E_{B-V}=0.76$ for V1425 Aql. With this estimate for reddening, the distance to the nova is 2.7 ± 0.6 kpc.

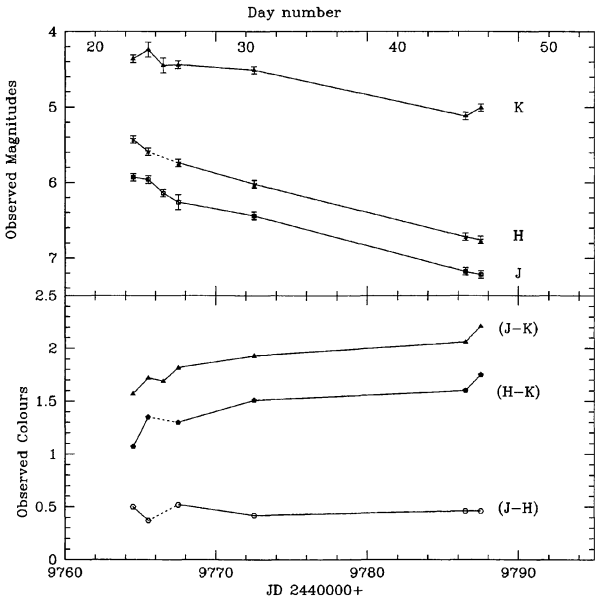

FIG. 2. *Top:* Observed *JHK* magnitudes of V1425 Aql as a function of time, $T_0 = 2449742.70$. The observations of May 18.93 are not shown here. Connecting lines are drawn as a visual aid. *Bottom:* Observed $J-H$, $H-K$ and $J-K$ color indices. Connecting lines are drawn as a visual aid.

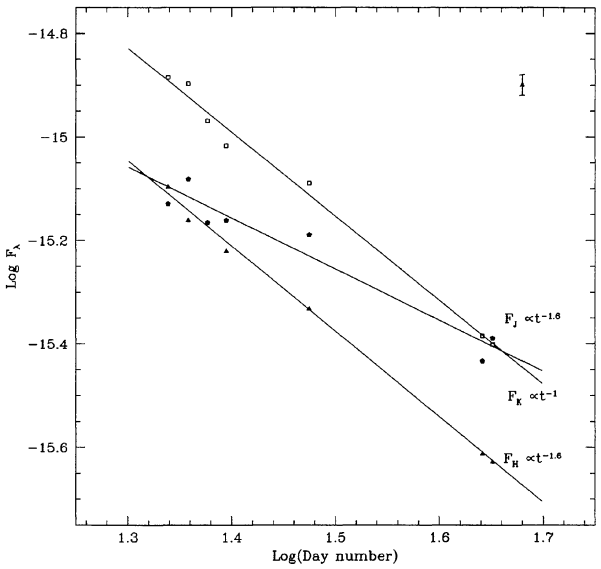

FIG. 3. Temporal evolution of the J (open squares), H (filled triangles), and K (filled pentagons) fluxes during days 22–45. Power laws suitable for the decline rate are also shown. F_λ is in units of W cm^{-2} μm^{-1}. Typical errorbar is shown on the upper right.

4. INFRARED PHOTOMETRY

JHK photometry was obtained with the 1.2 m telescope at the Mt. Abu Infrared Observatory using a LN_2-cooled InSb photometer. The details of the experimental system are given in Ashok *et al.* (1994). The first observations were obtained on 1995 February 16.02, eight days after discovery, and the monitoring continued until 1995 May 18.93. A 26 arcsec aperture was used, with a chopper throw of ~30 arcsec and a chopping frequency of 15 Hz. λ Aquilae (HR 7236), located close to the nova, was used as the standard star. Both the nova and the standard were observed alternately more than once on each night. The nova magnitudes were calculated with respect to the standard whose near-infrared magnitudes were obtained from Bouchet *et al.* (1991). Typical errors are ±0.05 mag, except for the K magnitudes on February 17.02 and 18.02 and J magnitude on February 19.02 which have an error of ±0.1 and the K magnitude on May 18.93 which has an error of ±0.2. The dates of observations and the observed *JHK* magnitudes are listed in Table 3, and the observed magnitudes and colors plotted in Fig. 2 for the period 1995 February–March.

The *JHK* fluxes, plotted in Fig. 3, indicate that the observed J and H fluxes fall off as $t^{-1.6(\pm 0.07)}$ whereas the observed K flux shows a slower decline of $t^{-1.0(\pm 0.11)}$ in the same time interval. These decline rates, in particular the K flux, are flatter than the expected rate of t^{-2} from an optically thin gas shell expanding with a constant thickness. This suggests the presence of optically thick components which could be in the form of continued mass loss, clumpy ejecta and/or dust. The presence of strong emission lines could also change the decline rate, but this would produce an erratic decline rather than the smooth decline observed here. The fact that the K flux shows a flatter decline compared to the J and H fluxes is indicative of the presence of dust. The observed color indices are red compared to other novae in the early post-maximum phase, e.g., nova V1974 Cyg (Ashok *et al.* 1992) or nova GQ Mus (Whitelock *et al.* 1984), but similar to those of novae which form dust, in particular nova V1668 Cyg (Gehrz *et al.* 1980b). A similar effect is seen even when the colors are corrected for the interstellar reddening using the estimated value of E_{B-V}, indicating that dust is indeed present in the system. In Table 4 we list for comparison the observed colors at dust shell maximum of other novae along with the observed colors of V1425 Aql on day 44.82.

From the observations of M96, we see that the K flux experienced a steep decline of $\sim t^{-4.2}$ between days 80 and 104. The overall decline rate, combining our data and that of M96, is $\sim t^{-2.6}$. A similar effect was seen in nova V838 Her after the dust shell maximum and has been attributed to destruction of the dust (Chandrasekhar *et al.* 1992; Harrison & Stringfellow 1994). Also, the L band magnitudes showed a sharp decline by nearly 1.75 mag between March 23.6 (day 57.4) and April 14.7 (day 79.5) (M96), thus pointing to the same cause. The J flux declined as $\sim t^{-1.9}$ after day 60, with an overall decline rate of t^{-2}, while the H flux declined as $t^{-2.8}$ after day 60 with an overall decline rate of $t^{-2.2}$. Figure 4 shows the overall temporal evolution of the fluxes in each of these bands.

The flux dependence $F_\lambda \propto t^{-2}$ is characteristic of gas ejected in a polar cone, equatorial disc configuration (Boyarchuk & Gershberg 1977), and the overall decline rate in V1425 Aql indicates a similar shell morphology.

5. PHYSICAL CONDITIONS

5.1 The Neutral Zone

Novae, particularly the "Fe II" novae, show an early appearance of the [O I] 6300, 6364 Å doublet, which together

TABLE 4. Comparison of IR colors with other dust forming novae.

Nova	$J-H$	$H-K$	$J-K$	Remarks
V1668 Cyg	1.2	1.7	2.9	Gehrz *et al.* 1980b
PW Vul	0.19	0.95	1.14	Gehrz *et al.* 1988
V838 Her	2.24	1.59	3.83	Chandrasekhar *et al.* 1992
V1419 Aql	1.84	2.24	4.08	Munari *et al.* 1994
V1425 Aql[1]	0.46	1.75	2.21	This paper

[1]Day 44.82.

with [N II] are the first forbidden lines to appear in the spectra. They are strong even after the appearance of high ionization lines such as [Fe VII]. The presence of the [O I] lines implies the presence of a neutral zone either as an envelope around the ionized gas or as dense condensations of neutral material embedded in an ambient ionized ejecta. The relative intensities of these lines are usually lower than the ratio of their transition probabilities when the lines are optically thin. This implies a high optical depth in the [O I] zone (Williams 1994). From the data presented here, we find the optical depth of the [O I] zone in V1425 Aql decreased from a value of 3.0 during Epoch I to 1.7 during Epoch III. The ratio of the [O I] lines 5577 Å and 6300 Å can be used to estimate T_e of the neutral zone (Williams 1994). The observed reddening corrected ratio of 6300/5577 in the early spectra yield an average temperature of 3800 K, consistent with values obtained in other novae. The neutral oxygen mass M_{O^0} estimated from the λ6300 line intensity varied from a value of $3.29\times10^{-4}\ M_\odot$ during Epoch I to $7.96\times10^{-5}\ M_\odot$ during Epoch III. The neutral oxygen mass had reduced considerably ($\sim10^{-9}\ M_\odot$) by day 843.

5.2 The Ionized Zone

5.2.1 Temperature, density, and mass

The [O III] λ4959+5007 to λ4363 ratio can be used to estimate the electron temperature (T_e) of the ionized zone. T_e during the early phases is estimated using the spectrum of 1995 April 7. Using the reddening corrected [O III] line ratios during this epoch, we obtain $T_e=9700$ K. We estimate T_e at the nebular phase as 1.2×10^5 K using the spectrum of 1997 May 17. Since the standard nebular lines used for density estimate are not available in our data, we use the Hβ luminosities to estimate the electron density n_e. The volume of the line emitting region is estimated assuming the shell to be spherical, uniformly expanding with an expansion velocity of 1300 km/s as deduced from the emission line widths (Wagner *et al.* 1995; Iijima *et al.* 1995; M96), and a filling factor of 0.1. The value of n_e varied as 10^8 cm^{-3} (Epoch I), 5×10^7 cm^{-3} (Epoch II), 1.7×10^7 cm^{-3} (Epoch III), and 3.8×10^5 cm^{-3} (Epoch IV). The mass of ionized hydrogen is estimated to be $6.5\times10^{-6}\ M_\odot$, $9.5\times10^{-6}\ M_\odot$, $1.2\times10^{-5}\ M_\odot$, and $1.1\times10^{-4}\ M_\odot$, at each of the epochs, respectively.

The total mass in the ejecta estimated from both the neutral and the ionized regions is $\sim10^{-4}\ M_\odot$.

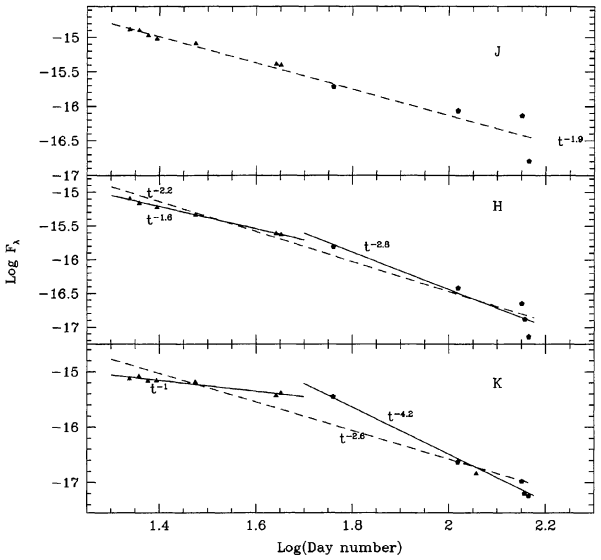

FIG. 4. *Top:* Temporal decline of the *J* flux over the days 22–147. Power law corresponding to the decline rate is shown. F_λ is in units of W cm^{-2} μm^{-1}. Filled triangles are our data and filled pentagons are data from M96. *Middle:* Temporal decline of the *H* flux. Power laws corresponding to the decline rates (see text) are shown. *Bottom:* Temporal decline of the *K* flux. Power laws corresponding to the decline rates (see text) are shown.

5.2.2 Elemental abundances

The elemental abundances in a nova ejecta may be estimated either using the plasma diagnostic approach or photoionization models. In either method, it is important to have spectra covering the ultraviolet, optical, and infrared regions for an accurate estimation of the elemental abundances using the ionic abundances of individual ions. The wavelength region covered by the data presented here is insufficient for an estimate of the abundances of all the elements and application of photoionization models. However, one may estimate the helium abundance

$$\frac{\mathrm{He}}{\mathrm{H}}=\frac{\mathrm{He}^+}{\mathrm{H}}+\frac{\mathrm{He}^{++}}{\mathrm{H}}$$

by the plasma diagnostic method (Osterbrock 1989), assuming pure radiative recombination. He^+ abundance is estimated using the ratios of 5876/Hβ and 6678/Hβ. The He I emissivities from Brocklehurst (1972) are corrected for collisional effects following Clegg (1987). He^{++} abundance is estimated using the He II 4686/Hβ ratio. The hydrogen and He II emissivities are from Hummer & Storey (1987). The data during Epoch III is very noisy around the He II 4686 line region. Hence the helium abundance is estimated using line intensities from Epochs I, II, and IV only. The estimates

TABLE 5. Helium element abundance.

Epoch	He^+/H	He^{++}/H	He/H
I	0.22	0.03	0.25
II	0.19	0.03	0.21
III	0.07	0.26	0.33

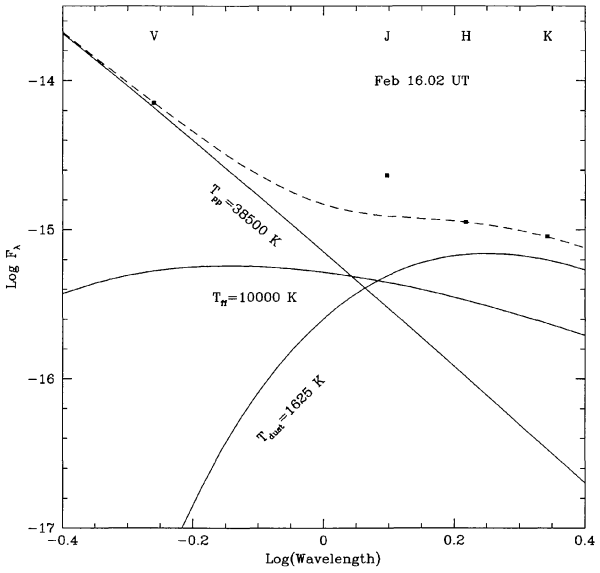

FIG. 5. Results of the model calculations for the observations of 1995 February 16. A pseudophotospheric temperature of 3.85×10^4 K and a free-free temperature of 10^4 K are assumed (see text for details of the model). The resulting dust temperature is 1625 K. Contributions from individual components are shown by solid lines, while the dashed line depicts the total of all contributions. Observed data are shown as filled squares. Note the prominent excess in the observed J flux over the model fit. Wavelength is in μm and fluxes (F_λ) in W cm^{-2} μm^{-1}.

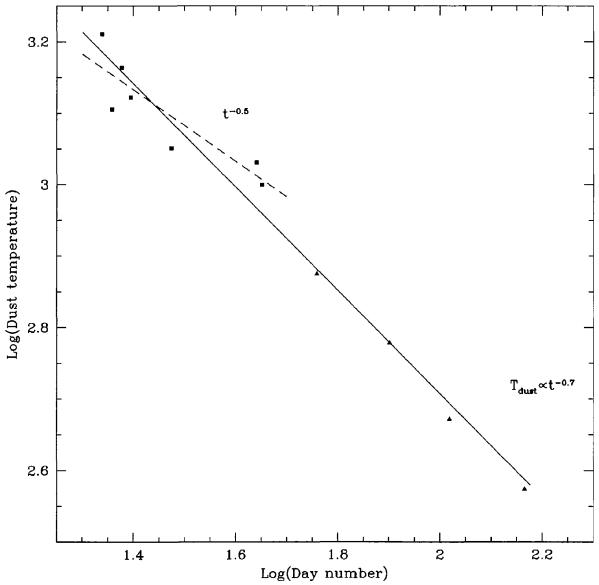

FIG. 6. Temporal evolution of dust temperature (T_d) estimated based on the model as described in the text. Filled squares correspond to our estimates and filled triangles correspond to the estimates from M96.

of He^+/H and those of He^{++}/H are listed in Table 5 for each of the epochs. A simple average of all the estimates of He/H gives the helium abundance in V1425 Aql as He/H=0.26 $\pm$0.06.

In the above approach, the electron temperature and density are assumed to be constant throughout the shell for each epoch. In the case of the nova PW Vul, Schwarz *et al.* (1997) have shown that such an assumption can underestimate the derived elemental abundances. However, in their analyses the discrepancy is the least for helium (10%).

6. DUST AND ITS NATURE

The IR data presented here indicate the presence of dust in the nova ejecta as early as day 22, the earliest observed dust formation timescale for an Fe II nova. However, no strong indication of dust formation process, such as a deep minimum in the visual light curve or rapid increase in the IR fluxes is observed. The optical depth of the dust shell is

$$\tau=(\lambda F_\lambda)_K/(\lambda F_\lambda)_V\sim0.02-0.04,$$

thus indicating that it was optically thin. The presence of [O I] lines along with lines of higher ionization in the optical spectrum is indicative of presence of clumps of neutral material which could be the zones of dust formation. Similar conclusion is also drawn by M96 based on IR spectra. Clumpy nature of the ejecta is conducive to early dust formation as seen in nova V838 Her (Chandrasekhar *et al.* 1992; Harrison & Stringfellow 1994).

The temperature of the dust is estimated from the *VJHK* fluxes, assuming contributions from the pseudophotosphere, ionized gas giving rise to free-free emission and the dust shell. The pseudophotosphere is that part of the optically thick envelope which moves inward in mass and thus becomes hotter with time during the post-maximum phase. The V magnitudes are estimated from the data available in the VSNET database as well as IAU Circulars. All fluxes have been dereddened using our estimate of $E_{B-V}=0.76$. The

TABLE 6. Model estimates of *VJHK* magnitudes and T_{dust}.

		Pseudophotosphere				Free-Free gas				Dust shell			
Day	T_{pp} 10^4 (K)	V	J	H	K	V	J	H	K	J	H	K	T_d (K)
21.82	3.85	6.94	7.51	7.65	7.71	9.67	7.10	6.37	5.61	7.00	5.60	4.54	1625
22.82	4.01	7.06	7.65	7.79	7.85	9.83	7.26	6.53	5.77	7.67	5.77	4.32	1275
23.82	4.03	7.08	7.67	7.81	7.87	9.88	7.30	6.57	5.81	7.43	5.82	4.58	1450
24.82	4.17	7.19	7.79	7.93	7.99	9.98	7.41	6.68	5.92	7.73	5.92	4.54	1325
29.84	4.60	7.52	8.13	8.27	8.34	10.26	7.69	6.96	6.20	8.29	6.19	4.58	1175
43.81	5.25	7.93	8.57	8.71	8.79	10.96	8.39	7.66	6.90	9.27	6.93	5.14	1075
44.82	5.38	8.01	8.65	8.80	8.88	11.00	8.43	7.70	6.94	9.52	6.97	5.01	1000

contribution of the individual components to the total flux in each of the bands is estimated in the following way. The free-free emitting region is assumed to be at a temperature of $T_{ff}=10^4$ K and contributing about 30% to the total flux in the H band, similar to the assumptions of Kenyon & Wade (1986) and Evans *et al.* (1990) for nova PW Vul. The psuedophotospheric contribution is estimated based on the temperature T_{pp} calculated using the expression

$$T_{pp}=15280\times 10^{\Delta m/7.5},$$

where Δm denotes magnitudes below maximum (Bath & Shaviv 1976). Accounting for these contributions to the total flux, we get the contribution from the dust, which is used to estimate the dust temperature T_d to within ± 25 K. The model fit with contribution from individual components for the data of February 16 (day 21.82) is shown in Fig. 5. A prominent excess is seen in the J band which could be due to emission lines.

Applying the model as described above, we find that T_d varied from 1625 K on day 21.82 to 1000 K on day 44.82. Table 6 gives the estimated values of T_d, T_{pp}, and *VJHK* magnitudes of each component. The estimate of $T_{pp}\sim 5.4\times 10^4$ K on day 45 is comparable with the value of 9×10^4 estimated for nova V443 Sct on day 77 (Anupama *et al.* 1992).

The value of T_d is most sensitive only to the free-free contribution. Changing the free-free contribution in the H band by $\pm 20\%$ results in a change in T_d by about 100 K. An error in estimating the V magnitude by ± 0.1 mag changes the estimated photospheric temperature by ± 2000 K. However, T_d remains insensitive even to a change in the photospheric temperature by ± 5000 K due to the low photospheric contribution in the IR.

Applying our model to the data of M96 on March 23.6 (day 57.4), we estimate T_d to be 850 K, compared to their estimate of 750 K. It should be noted here that our estimate is based only on the *JHK* fluxes and within errors, compares well with M96. T_d declined as $t^{-0.5\pm 0.07}$ during the period of our observations. A $t^{-0.5}$ decline rate is expected in the case of clumps moving away from the central source at a constant velocity. The M96 data gives a decline rate of $t^{-0.75\pm 0.03}$ and the overall decline rate, using our data as well as those of M96, is $t^{-0.72\pm 0.04}$. Figure 6 shows the temporal evolution of the dust temperature. The estimated dust temperature for V1425 Aql is similar to that observed in other novae.

The dust temperature, early dust formation and the blackbody-like spectral energy distribution in the near-IR are all indicative of the dust being composed of carbon grains (Clayton & Wickramasinghe 1976). Following Gehrz *et al.* (1980a) and assuming the carbon grains have a density of ~ 2.2 g cm^{-3} and are ≤ 1 μm in size, we estimated the mass of the dust during our period of observations using the K band flux of the dust shell as estimated by the model (see Table 6). The dust mass increased from a value of 6.01×10^{-10} $M_\odot$ on day 21.82 to 7.22×10^{-9} $M_\odot$ by day 44.82. These values are a lower limit to the mass of the condensable matter as there could be some uncondensed material in the ejecta. The dust to gas ratio during this period is $0.1-1.2\times 10^{-3}$, where we have used a value of 6×10^{-6} $M_\odot$ for the mass of the gas, as estimated from the optical spectra during Epoch I. It may be noted here that the gas mass used is that of ionized hydrogen. However, the mass of gas in the neutral zone where the dust is expected to be formed could be higher, as is seen from the estimate of mass in the neutral oxygen zone, and the above estimated dust-to-gas ratio would be further lower. M96 obtain a dust mass of 8×10^{-7} $M_\odot$ and a dust to gas ratio of 2.5×10^{-3} from their 1995 June observations.

We require the grains to have grown 4.4 times in size while reducing 7 times in number between days 22 and 45 to account for our observations, assuming that the source maintained a constant luminosity in the dust formation period. Any probable change in the source luminosity will modify this conclusion.

TABLE 7. Summary of derived physical parameters.

Parameter	Value	Method
T_0	JD 2449742.70	light curve, optical spectra
t_2	11 days	V light curve
t_3	23 days	V light curve
v_{ej}	1300 km s^{-1}	spectra
M_V^{max}	-8.4 ± 0.4	MMRD relations
E_{B-V}	0.76	HeI line ratio
D	2.7 ± 0.6 kpc	E_{B-V} & M_V^{max}
L	$1.49\times 10^5 L_\odot$	M_V^{max}
$T_{neutral\ zone}$	3800 K	optical spectra
$T_{ionized\ zone}$	120000 K[a]	optical spectra
M_{H^+}	$1\times 10^{-4} M_\odot$[a]	optical spectra
M_{O^0}	$3\times 10^{-4} M_\odot$[b]	optical spectra
N(He)/N(H)	0.26 ± 0.06	optical spectra
T_d	1625 K[c]	*JHK* photometry
τ_{dust}	$\sim 0.02-0.04$[d]	V and K data
M_{dust}	$0.6-7.22\times 10^{-9} M_\odot$[d]	IR data
Dust/gas	$\lesssim 10^{-3}$	

[a]Day 843.8.
[b]Day 50.5.
[c]Day 21.82.
[d]Day 21.82–44.82.

7. FINAL REMARKS

The early postmaximum and nebular spectra in the optical region and infrared magnitudes are presented. The spectra of V1425 Aql indicate it belongs to the Fe II class of novae and was discovered nearly two weeks past maximum. The spectrum and its evolution in the optical region is quite similar to novae belonging to the Fe II class. The nova outburst was accompanied by formation of optically thin carbon dust. Dust formation occurred as early as 22 days past maximum and appears to be unique to the Fe II class of novae in which dust formation has been observed. The mass of the dust is very low, with a dust-to-gas ratio $\lesssim 10^{-3}$. Dust appears to have formed in clumps of neutral material embedded in an ionized gas. This nova also developed infrared coronal lines at a later phase (M96) making it a transition between the dusty novae and the coronal novae.

We summarize in Table 7 some of the important physical parameters estimated in this work.

We thank the assistants on duty at the VBT for their help during observations and for obtaining the data on 1995 April 7. G.C.A. thanks T.P. Prabhu for valuable suggestions. Research work at PRL is supported by the Department of Space, Government of India. IRAF is distributed by National Optical Astronomy Observatories which is operated by the Association of Universities Inc. (AURA) under cooperative agreement with the National Science Foundation, U.S.A.

REFERENCES

Anupama, G. C., Duerbeck, H. W., Prabhu, T. P., & Jain, S. K. 1992, A&A, 263, 87
Ashok, N. M., Chandrasekhar, T., & Ragland, S. 1992, IAU Circ., No. 5525
Ashok, N. M., Chandrasekhar, T., Ragland, S., & Bhatt, H.C. 1994, Experimental Astronomy, 4, 177
Bath, G. T., & Shaviv, G. 1976, MNRAS, 175, 305
Bouchet, P., Manfroid, J., & Schmider, F. X. 1991, A&AS, 91, 409
Boyarchuck, A. A., & Gershberg, R. E. 1977, Sov. Astron., 21, 275
Brocklehurst, M. 1972, MNRAS, 157, 261
Capaccioli, M., Della Valle, M., D'Onofrio, M., & Rosino, L. 1989, AJ, 97, 1622
Chandrasekhar, T., Ashok, N. M., & Ragland, S. 1992, MNRAS, 255, 412
Clayton, D. D., & Wickramasinghe, N. C. 1976, ApSS, 42, 263
Clegg, R. E. S. 1987, MNRAS, 229, 31p
Cohen, J. G. 1985, ApJ, 292, 90
Duerbeck, H. W. 1981, PASP, 93, 165
Evans, A., Callus, C. M., Whitelock, P. A., & Laney, D. 1990, MNRAS, 246, 527
Gehrz, R. D., Grasdalen, G. L., Hackwell, J. A., & Ney, E. P. 1980a, ApJ, 237, 855
Gehrz, R. D., Hackwell, J. A., Grasdalen, G. L., Ney, E. P., Neugebauer, G., & Sellgren, K., 1980b, ApJ, 239, 570
Gehrz, R. D., Harrison, T. E., Ney, E. P., Matthews, K., Neugebauer, G., Elias, J., Grasdalen, G. L., & Hackwell, J. A. 1988, ApJ, 329, 894
Greeley, B. W., Blair, W. P., & Long, W. S. 1995, ApJL, 454, L43
Harrison, T. E., & Stringfellow, G.S. 1994, ApJ, 437, 827
Hummer, D. G., & Storey, P.J. 1987, MNRAS, 224, 801
Iijima, T., Esenoglu, H., & Rosino, L. 1995, IAU Circ., No. 6135
Kenyon, S. J., & Wade. R. A. 1986, PASP, 98, 935
Mason, C. G., Gehrz, R. D., Woodward, C. E., Smilowitz, J. B., Greenhouse, M. A., Hayward, T. L., & Houck, J. R. 1996, ApJ, 470, 577 (M96)
Munari, U., Yudin, B. F., Kolotilov, E. A., Shenavrin, V. I., Sostero, G., & Lepardo, A. 1994, A&A, 284, L9
Nakano, S. 1995, IAU Circ., No. 6133
Neckel, Th., & Klare, G. 1980, A&AS, 42, 251
Ohshima, O., Shimizu, M., Ayani, K., & Suzuki, M. 1995, IAU Circ., No. 6154
Osterbrock, D. E. 1989, Astrophysics of Gaseous Nebulae and Active Galactic Nuclei (University of Science, Mill Valley)
Prabhu, T. P., Anupama, G. C., & Surendiranath, R. 1997, Bull. Astr. Soc. India (in press)
Schwarz, G. J., Starrfield, S. G., Shore, S. N., & Hauschildt, P. 1997 (preprint)
Wagner, R. M., Bertram, R., & Starrfield, S. G. 1995, IAU Circ., No. 6134
Whitelock, P. A., Carter, B. S., Feast, M. W., Glass, I. S., Laney, D., Menzies, J. W., Walsh, J., & Williams, P. M. 1984, MNRAS, 211, 421
Whitney, B. A., & Clayton, G. C. 1989, AJ, 98, 297
Williams, R. E. 1992, AJ, 104, 725
Williams, R. E. 1994, ApJ, 426, 279
Williams, R. E., Hamuy, M., Phillips, M. M., Heathcote, S. R., Wells, L., & Navarrete, M. 1991, ApJ, 376, 721
Williams, R. E., Phillips, M. M., & Hamuy, M. 1994, ApJS, 90, 297